

# Molecular modeling of flexible molecules. Vapor–liquid and fluid–solid equilibria

C. Vega<sup>a,\*</sup>, L.G. MacDowell<sup>a</sup>, C. McBride<sup>a</sup>, F.J. Blas<sup>b</sup>, A. Galindo<sup>c</sup>, E. Sanz<sup>a</sup>

<sup>a</sup>Departamento de Química Física, Facultad de Ciencias Químicas, Universidad Complutense, 28040, Madrid, Spain

<sup>b</sup>Departamento de Física Aplicada, Escuela Politécnica Superior, Universidad de Huelva, 21819 La Rábida, Huelva, Spain

<sup>c</sup>Department of Chemical Engineering and Chemical Technology, Imperial College of Science, Technology and Medicine, Prince Consort Road, London SW7 2BY, UK

## Abstract

We consider recent applications of Wertheim's first order perturbation theory (TPT1) to the description of the critical properties and the freezing transition of chain molecules. Firstly we consider an extension of TPT1 which allows one to describe the equation of state of atomistic molecular models which incorporate fine chemical details such as overlap between the sites, fixed bond angles and torsional potentials. The theory is applied to the description of the critical properties of all isomers ranging from butane to octane and good qualitative agreement is found. We then show how TPT1 may be applied to the description of the freezing transition of chain molecules. We apply the theory to chains of tangent hard spheres and Lennard–Jones chains and find good agreement for the equation of state and free energies of the fluid and solid phases. Fluid–solid coexistence properties predicted by the theory are in close agreement with simulation results. It is shown that for hard sphere and Lennard–Jones dimers the stable solid structure is a disordered one, with the atoms forming a close packed arrangement, but with the bonds distributed randomly within the solid.

© 2004 Elsevier B.V. All rights reserved.

**Keywords:** Statistical thermodynamics; Wertheim's theory; Monte Carlo simulations; Alkanes

## 1. Introduction

Some time ago Wertheim presented a very successful theory to study the thermodynamic properties of hard-core fluids interacting via short-range attractive (association) forces [1–4], such as hydrogen bonding fluids. When the association strength becomes infinitely strong chains are formed from a fluid of associating monomers [5]. Therefore Wertheim theory can be used to describe the thermodynamic properties of chain models. In the simplest implementation of the theory, which is commonly denoted as the first order thermodynamic perturbation theory (TPT1), the only information required in order to build an approximate equation of state for the chain fluid is the equation of state of the monomer fluid, together with its pair correlation function at contact. The equation of state (EOS) for hard sphere chains arising from TPT1 was proposed independently by Wertheim

[6] and by Chapman et al. [7]. The theory can be extended to systems where the monomer–monomer interaction presents an attractive contribution as is the case for the Lennard–Jones (LJ) model [8,9], the square well potential [10] and the Yukawa potential [11]. In this way it has been possible to derive equations of state (EOS) for freely jointed tangent chains (formed by tangent monomers with no constraint in the bonding angle or torsional state). The theory has been quite successful in describing a number of properties of models formed by tangent monomers (see the excellent review of Muller and Gubbins for additional references [12]).

Let us summarize briefly the main equations of Wertheim's TPT1. Let us assume that we have a certain number,  $N^{\text{ref}}$ , of spherical monomer particles within a certain volume  $V$  at temperature  $T$ , and that these particles interact through a spherical pair potential  $u^{\text{ref}}(r)$ . We denote this fluid as the reference fluid and the properties of this reference fluid will be labeled by the superscript ref. Let us also assume that in another

\*Corresponding author. Tel.: +34-91-394-42-02; fax: +34-394-41-35.

E-mail address: cvega@guim.sim.ucm.es (C. Vega).

container of volume  $V$  and temperature  $T$ , we have  $N = N^{\text{ref}}/m$  fully flexible chains of  $m$  monomers each. Each monomer of a certain chain interacts with all the other monomers in the system (i.e. in the same molecule or in other molecules with the only exception being the monomer/s to which it is bonded) with the pair potential  $u^{\text{ref}}(r)$ . The chain system described so far will be denoted as the chain fluid. By fully flexible chains we mean that there is neither bending nor torsional potentials between the monomers of the chain. The only intramolecular interaction is the presence of a pair potential between monomers of the same chain separated by more than one bond. In this case, the free energy of the chain fluid as given by the TPT1 theory is [1–19]:

$$\frac{A}{NkT} = \ln(\rho \Lambda^3) - 1 + m \frac{A_{\text{residual}}^{\text{ref}}}{N^{\text{ref}}kT} - (m-1) \ln y^{\text{ref}}(\ell). \quad (1)$$

where  $\rho = N/V$  is the number density of chains,  $\Lambda$  is the thermal de Broglie wavelength,  $A_{\text{residual}}^{\text{ref}}$  is the residual free energy of a fluid of free monomers interacting with the reference potential, while  $y^{\text{ref}}(\ell)$  is the background correlation function [20] evaluated at the bonding distance  $\ell$ . The equation of state which follows from Eq. (1) is given by

$$Z = mZ^{\text{ref}} - (m-1) \left( 1 + \rho^{\text{ref}} \frac{\partial \ln y^{\text{ref}}(\ell)}{\partial \rho^{\text{ref}}} \right), \quad (2)$$

As can be seen, according to the above equations all that is needed to obtain the free energy of the chain fluid is the residual free energy of the reference monomer system (at the same  $T$  and monomer density) and the contact value of the background correlation function of the monomer reference fluid (both properties of the reference fluid obtained at the same  $T$  and monomer number density as the chain fluid). We denote Eqs. (1) and (2) as Wertheim's TPT1 theory. Despite the success of TPT1 in describing the equation of state of polymer fluids and their mixtures, there are still some problems that cannot or have not yet been addressed by this theory. We shall address two of such problems in this work.

Chain molecules found in nature, such as alkanes, present high overlap of the interaction sites, an almost constant bond angle and a torsional potential governing the motion of the chain along the bond vectors. These fine chemical details which very much affect the equation of state cannot be incorporated in a clear manner into TPT1, since it was originally designed for tangent monomer models. Another related problem is the effect of branching. For an homopolymer TPT1 does not distinguish between branched and non-branched isomers. It is therefore questionable that the original TPT1 can be used to obtain differences between the thermo-

dynamic properties of branched and non-branched isomers. Obviously, one could still use TPT1 for branched and non-branched isomers by using adjustable potential parameters for each isomer. This approach although useful for practical applications (to reproduce experimental results) is not so useful if one wishes to understand and explain the origin of the difference in properties of branched and non-branched alkanes. In the first part of this paper, we will describe a methodology that it is able to extend TPT1 in order to describe molecules with arbitrarily complex chemical details. This will permit a description of the effect of branching on the critical properties of alkane isomers.

Another interesting problem is the freezing transition of chain molecules. Quite recently we have noticed [21] that the arguments used to arrive to Eqs. (1) and (2) make no special mention as to the actual nature (i.e. fluid or solid) of the phase considered. The question is then: could we use Eqs. (1) and (2) to describe the solid phase of fully flexible chains? This is an interesting question which has also important practical consequences. Actually, many flexible molecules exhibit a stable solid phase at room temperature and pressure. For instance, all linear alkanes with more than 20 carbon atoms are solid at room temperature and pressure, and the same is true for polyethylene [22]. In many industrial processes one has to deal with the fluid–solid separation of alkane mixtures. Therefore, a theoretical description of the solid phase of flexible chain molecules would be of great interest both from a fundamental and a practical point of view and the interest in the area is just starting [23]. In a series of studies we have compared the results from Wertheim's TPT1 as applied to the solid phase to simulation results. In Ref. [21] it was shown that Wertheim's TPT1 describes quite well the EOS of hard sphere chains from  $m=3$  up to  $m=8$ . In Ref. [24] it was shown that Wertheim's TPT1 also describes quite well the EOS of two-dimensional disk dimers. Also, recently [25] it has been shown that Wertheim's TPT1 predicts quite well the EOS and internal energy of the LJ dimer in the solid phase. In these studies, however, it was not possible to compare the free energies from Wertheim's theory to those of simulation. It is our goal here to determine free energies for some of these models in the solid phase, and to compare the predictions from Wertheim's TPT1 to the simulation results. For that purpose we have chosen the dimer model with two monomer sites  $m=2$ . For this model, the determination of the free energy of the solid phase via computer simulation is relatively straightforward. In fact, for the hard dumbbell tangent dimer, previous calculations of the free energy were available for the 'ordered' structures [26]. This work sets out to determine the free energy of the dimer model for the true equilibrium 'disordered' structure, and to prove that the disordered structure is indeed more stable than the ordered structure for the

dimer model. Also, we determine the free energies of the LJ dimer in the solid phase, for the ordered and for the disordered structures, and to establish again clearly that the disordered structure is indeed more stable than the ordered one.

This paper illustrates how Wertheim's TPT1 can be used for problems different from those for which it was originally designed. The scheme of the paper is as follows. In Section 2 we shall show how Wertheim's TPT1 when modified properly can provide a qualitative view of the variation of the critical properties of alkanes (linear and branched). In Section 3, results of Wertheim's TPT1 for several dimer models in the solid phase will be presented, with special emphasis in the free energy as determined from theory and from simulation. Finally, in Section 4 the main conclusions of this work will be presented.

## 2. Liquid–vapor phase coexistence of short alkanes

### 2.1. Model alkane

We describe the alkanes by means of a united atom model. The groups  $\text{CH}_3$ ,  $\text{CH}_2$ ,  $\text{CH}$  and  $\text{C}$  will be represented by a Lennard–Jones (LJ) interaction site located on the position of the carbon atom. The number of carbon atoms of the alkane will be denoted by  $n$ . These interaction sites are responsible for all of the intermolecular interactions and for those intramolecular interactions, which take place between atoms more than three bonds apart. The potential governing interactions between sites  $i$  and  $j$  is taken to be of the Lennard–Jones type:

$$u(r_{ij}) = 4\varepsilon_{ij} \left[ \left( \frac{\sigma_{ij}}{r_{ij}} \right)^{12} - \left( \frac{\sigma_{ij}}{r_{ij}} \right)^6 \right] \quad (3)$$

A different value for  $\varepsilon$  and  $\sigma$  will be assigned to the  $\text{CH}_3$ ,  $\text{CH}_2$ ,  $\text{CH}$  and  $\text{C}$  groups. Crossed interactions between different groups are considered to obey the Lorentz–Berthelot rules [27]. The actual values we have considered for  $\varepsilon$  and  $\sigma$  are set II of Ref. [28]. The carbon carbon bond distance is taken as  $l = 1.53 \text{ \AA}$ , while the C–C–C bond angle  $\theta$  is set to the tetrahedral value, i.e.  $\theta = 109.5$ . The flexible nature of the molecule is introduced at the level of the torsional degrees of freedom. More specifically, we consider that the overall potential about a given bond vector is the sum of  $n$ -butane torsional potentials of the Ryckaert–Bellemans form [29] for each possible dihedral angle.

### 2.2. Perturbation theory

The Helmholtz free energy  $A$  is given by the sum of ideal, intra-molecular and intermolecular contributions.

Owing to the flexible nature of the molecules, these two last contributions depend on molecular parameters which are themselves a function of the conformational population,  $\mathbf{X}$ , of the system. The free energy then becomes a functional of  $\mathbf{X}$ . In order to simplify the problem, we consider the rotational isomer approximation (RIS) [30]. In this way, the continuum of torsional angles is replaced by a discrete set of three torsional states, *trans*, *gauche* + and *gauche* –, so that the conformational space is discretized. The Helmholtz free energy may be then expressed as:

$$A = A_{\text{ideal}} + A_{\text{intra}}(\mathbf{X}) + A_{\text{inter}}(\mathbf{X}) \quad (4)$$

where  $\mathbf{X} = (x_1, x_2, \dots, x_q)$  is now a vector whose components are the molar fractions of the conformers of the system (the number of possible conformers may be large but remains finite within the RIS approximation).

The ideal term is simply given by:

$$A_{\text{ideal}}/Nk_B T = \ln(\rho \Lambda^3) - 1 \quad (5)$$

The intramolecular term is given within the RIS approximation by [30–32]:

$$A_{\text{intra}}/N = k_B T \sum_{i=1}^{i=q} x_i \ln(x_i) + \sum_{i=1}^{i=q} x_i n_{g,i} E_1 + \sum_{i=1}^{i=q} x_i U_{\text{intra},i}(\text{LJ}) \quad (6)$$

where  $n_{g,i}$  is the number of *gauche* bonds of conformer  $i$ ,  $U_{\text{intra}}(\text{LJ})$  is the intramolecular LJ energy of conformer  $i$ ,  $q$  is the number of possible conformers of the molecule, and  $E_1$  is the torsional energy of a torsional bond in the *gauche* state (the energy of the *trans* state is taken as zero).

As to the intermolecular contribution, we will consider a first order perturbation theory. The total configurational energy of the system is divided into purely intramolecular and purely intermolecular parts. The latter part is made up of the sum of all interactions between sites of different molecules. The intermolecular site–site potential is then decomposed into a repulsive term,  $u_0$ , and an attractive term,  $u_1$ , following the Weeks–Chandler–Andersen decomposition. The repulsive reference term is obtained from the full LJ potential as follows:

$$u_0^{kl}(r) = \begin{cases} 4\varepsilon_{kl} \left[ \left( \frac{\sigma_{kl}}{r} \right)^{12} - \left( \frac{\sigma_{kl}}{r} \right)^6 \right] + \varepsilon_{kl} & r \leq 2^{1/6} \sigma_{kl} \\ 0 & r > 2^{1/6} \sigma_{kl} \end{cases} \quad (7)$$

while the attractive perturbation term is obtained as  $u_1 =$

$u - u_0$ . The complete reference system is made up of all the intramolecular interactions, plus the repulsive intermolecular interactions, while the perturbation contains all of the intermolecular attractive interactions. In this way, the conformational population of the reference system is the same as that of the full system in the ideal gas limit.

When the interaction potential is so divided, the configurational contribution to the Helmholtz free energy may be split into two terms:

$$A_{\text{inter}}(\mathbf{X}) = A_0(\mathbf{X}) + A_1(\mathbf{X}) \quad (8)$$

where  $A_0(\mathbf{X})$  is the intermolecular free energy of the reference system when the population of conformers is given by the actual population of the full system,  $\mathbf{X}$ , while  $A_1(\mathbf{X})$  is the intermolecular free energy due to the perturbation potential.

In order to obtain an explicit expression for  $A_0$ , we will require an approximation which consists in assigning an effective hard body to the reference system. In this work we will assume that a WCA site of type  $i$  may be mapped into a hard sphere site with an effective diameter [28,33]. Once an effective hard body has been assigned to the reference system, we still need an equation of state to describe a rather complex molecular fluid made of overlapping hard spheres with fixed bond angles and torsional potentials. Although this is in principle an extremely complicated problem, we have found that an empirical modification of Wertheim's perturbation theory works very well. Our approach consists in modifying the original expression for chains of tangent hard spheres [6–8] so that it predicts the correct second virial coefficient of the molecule under consideration. Similar modifications were proposed some time ago [34,35]. This approach, which we call Modified Wertheim Theory (MWT), has been shown to yield excellent results for hard linear and branched alkanes [31,32,36,37]. The resulting expression for the free energy reads [31]:

$$\frac{A_0}{Nk_B T} = (2\bar{\alpha} - 1) \ln \left( \frac{2(1-y)^3}{(2-y)} \right) - (2\bar{\alpha} - 2) \frac{1+y-0.5y^2}{(1-y)(1-0.5y)} \quad (9)$$

where  $\bar{\alpha}$  is the average non-sphericity parameter of the molecule and the packing fraction,  $y$ , is given as the product of the number density and the average molecular volume,  $\bar{V}$ . Comparison of this equation with the original expression shows that our approach amounts to finding an effective number of tangent hard spheres,  $m_{ef}$ , which is related to  $\bar{\alpha}$  by  $m_{ef} = 2\bar{\alpha} - 1$ . More details of this approach may be found elsewhere [31,32,36,37].

Eq. (9) can be summarized by saying that when describing the 'realistic' hard alkane model, we used Wertheim's TPT1 for an idealized model of  $m_{ef}$  tangent hard spheres. The parameter  $m_{ef}$  is determined by imposing that the second virial coefficient of the 'realistic' hard alkane is equal to that of the flexible tangent hard sphere model (as given by the original Wertheim's TPT1 for tangent hard spheres).

The perturbative contribution to the Helmholtz free energy may be determined by means of the following equation:

$$A_1/Nk_B T = \frac{1}{2} \beta \rho \sum_{k=1}^n \sum_{l=1}^n \int u_1^{kl}(r) g_{0,kl}(r; \rho) 4\pi r^2 dr \quad (10)$$

where  $g_{0,kl}$  is the site-site correlation function between sites  $k, l$  of the reference system. Eqs. (4)–(6), (8)–(10) constitute a general expression for the free energy of flexible molecules where the conformational population is obtained variationally from the total free energy of the system [31,32,38]. The approach is, however, rather involved and will not be considered here. In this work we will henceforth assume that the conformational population is given by the ideal gas limit and does not change with density. Although this approximation does not hold for long chains, it is quite accurate for the short alkanes that will be considered here [31,32,39–41]. In this way, the intramolecular contribution is a constant for a given temperature and may be altogether ignored for the purpose of phase equilibria calculations.

Even within this approximation, the calculation of  $g_{0,kl}$  for arbitrary densities is a very complicated and time consuming problem. We will therefore consider a van der Waals approximation, whereby the site-site correlation functions are assumed to be density independent and equal to the site-site correlation functions at zero density. In this way,  $A_1$  becomes a simple linear function of the density which takes the following form:

$$A_1/Nk_B T = -\beta a_{\text{vdw}} \rho \quad (11)$$

In the above equation,  $a_{\text{vdw}}$  is a van der Waals constant, which is determined by integration of the zero density site-site correlation functions of the reference system,  $g'_{0,kl}$ :

$$a_{\text{vdw}} = - \sum_k^n \sum_l^n 2\pi \int_{d_{kl}}^\infty u_1^{kl}(r) g'_{0,kl}(r, \mathbf{X}^{si}) r^2 dr \quad (12)$$

As to the zero density site-site correlation functions, they are determined numerically by means of an efficient algorithm proposed recently, which is based on the idea that  $g'_{0,kl}$  may be considered to be a Mayer function with molecular reference frames placed on sites  $k, l$  [42]. The argument  $\mathbf{X}^{si}$  emphasizes that  $g'_{0,kl}$  is obtained as

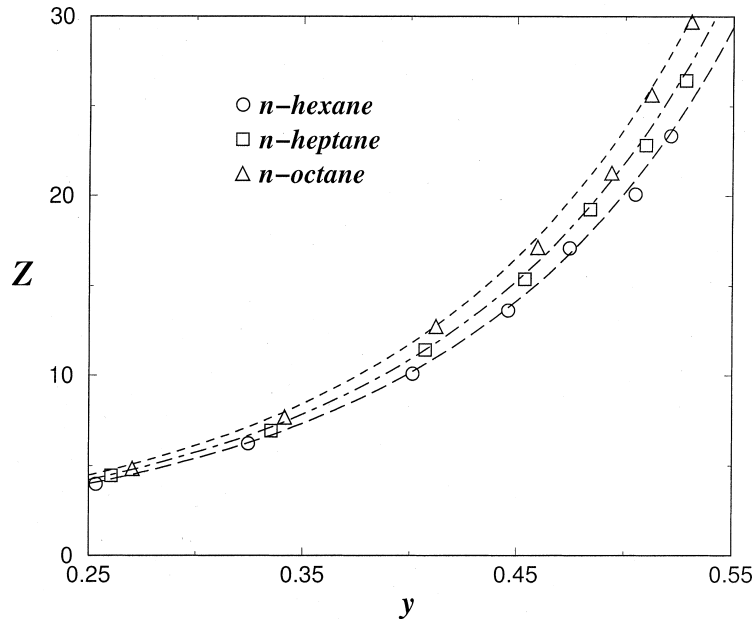


Fig. 1. Compressibility factor  $Z$  for hard  $n$ -alkane chains as a function of packing fraction. Symbols, simulation results. Lines, theoretical predictions from Wertheim TPT1 using an effective number of tangent spheres  $m_{ef}$ . All interaction sites associated to each carbon atom have a hard sphere of diameter  $d=3.7109$  Å.

an average of pairs of conformers sampled from an ideal gas population.

To summarize, the final expression for the Helmholtz free energy that we will consider is then given by the sum of Eqs. (5), (9), (11) and (12). More explicitly, it takes the form:

$$\frac{A_0}{Nk_B T} = \ln(\rho \Lambda^3) - 1 + (2\bar{\alpha} - 1) \ln \left( \frac{2(1-y)^3}{(2-y)} \right) - (2\bar{\alpha} - 2) \frac{1+y-0.5y^2}{(1-y)(1-0.5y)} - \beta a_{vdw} \rho \quad (13)$$

where  $y = \mathcal{V} \rho$ , while  $\alpha$ ,  $\mathcal{V}$  and  $a_{vdw}$  are molecular parameters determined as conformational averages from the ideal gas population. Since we regard the system as a multicomponent mixture of rotational isomers,  $\bar{\alpha}$  and  $\bar{\mathcal{V}}$  are given by:

$$\bar{\alpha} = \sum_{i=1}^q x_i \alpha_i \quad (14)$$

$$\bar{\mathcal{V}} = \sum_{i=1}^q x_i \mathcal{V}_i \quad (15)$$

where the sum runs over all possible conformers, while the molar fractions of the conformers are assumed to be those found in the limit of zero density. In principle, the values of  $\alpha_i$  needed in the previous equation may be

obtained from a knowledge of the second virial coefficients. However, this requires rather time consuming calculations. For that reason, instead of evaluating the second virial coefficient we shall use a method recently proposed (based on convex body geometry) that yields accurate and quick predictions of the second virial coefficient of chains with up to 100 monomer units [36,42].

### 2.3. Results

#### 2.3.1. Test of the reference equation of state

Before we consider the predictions of the mean field equation of state that we have proposed, it is convenient to test the performance of the reference equation of state employed to describe the repulsive alkane models. In Fig. 1 we show the compressibility factor of hard linear model alkanes, ranging from  $n$ -hexane to  $n$ -octane, as a function of packing fraction. The lines are results obtained from MWT, while the symbols are Monte Carlo simulation results. The figure shows rather good agreement between simulation and theory, even for packing fractions as high as 0.55, close to the expected freezing transition [43]. Although MWT was originally devised for linear alkanes [31,32,36], we have recently shown that it is also very accurate for branched alkanes [37,44]. In Fig. 2 we show the equation of state for three isomers of octane, namely,  $n$ -octane, 2,5-dimethylhexane and 2,2,3,3-tetramethylbutane. It is seen that the theory yields good results for all three substances, and that choosing  $m_{ef}$  as discussed previously allows one to

clearly describe the effect of branching on the equation of state of different alkane isomers. Such an effect is seen to be quite pronounced. Indeed, by comparing Fig. 1 with Fig. 2 it is seen that the differences in the compressibility factor of octane isomers may be considerably larger than those observed by changing the actual number of carbon atoms in the chain. In order to see this more clearly, Table 1 presents the results of the effective number of spheres for the different substances considered in this work. As expected, the effective chain length of *n*-alkanes increases as the number of carbon atoms increases. For branched alkanes, however, the effective chain length no longer shows such a simple dependence. Usually, the more heavily branched the alkane, the smaller its effective chain length will be. Although this qualitative statement is rather intuitive, quantification is another matter. Table 1 presents a quantitative statement of this fact. It is seen that the effect of branching is such that 2,5-dimethylhexane is effectively a shorter chain than *n*-heptane, while 2,2,3,3-tetramethylbutane is effectively shorter than *n*-hexane. This will obviously have a very significant effect on the critical properties of branched alkanes.

### 2.3.2. Critical properties of branched alkanes

Now that the equation of state for the reference fluid has been tested we may consider the predictions from the mean field theory more confidently. We note, however, that one cannot expect a quantitative agreement

Table 1

Effective chain length  $m_{ef}$  and molecular volume  $\mathcal{V}$  (in units of  $d^3$ , the diameter of the hard sphere associated to each monomer) for some hard alkane models. The value of the hard sphere diameter associated to each monomer is  $d=3.7109$  Å

Alkane	$m_{ef}$	$\mathcal{V}$
<i>n</i> -hexane	1.76838	2.027161
<i>n</i> -heptane	1.94843	2.326571
<i>n</i> -octane	2.15632	2.625892
2,5-dimethylhexane	1.89752	2.610603
2,2,3,3-tetramethylbutane	1.47211	2.569577

from the theory, due to the van der Waals approximation employed for the perturbative contribution, which has the effect of considerably underestimating the intensity of the site–site correlations. As an example, for the critical temperature this would have the effect of considerably underestimating the experimental result. For this reason, instead of performing a direct comparison between theory and experiment, we rescale the theoretical results for a given alkane isomer by a factor such that the theory yields exact results for the corresponding *n*-alkane of that family. For example, in case of the critical temperatures of a hexane isomer, we plot a rescaled critical temperature,  $T'_i$ , obtained as follows:

$$T'_i = \frac{T_{n\text{-hex}}^{\text{exp}}}{T_{n\text{-hex}}^{\text{the}}} T_i^{\text{the}} \quad (16)$$

where  $T_{n\text{-hex}}^{\text{exp}}$  is the experimental critical temperature of

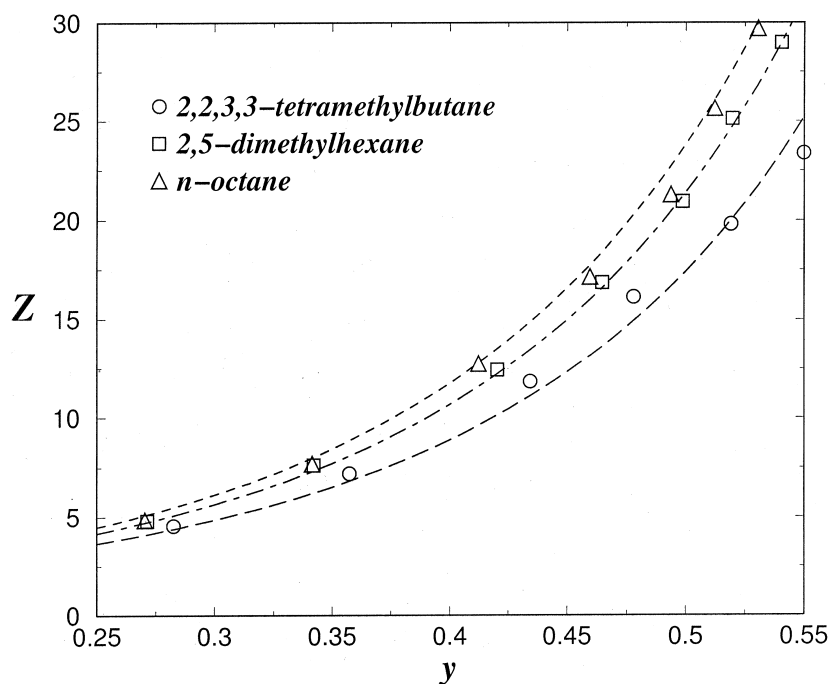


Fig. 2. Compressibility factor  $Z$  for three different hard octane isomers as a function of packing fraction. Symbols, simulation results. Lines, theoretical predictions from Wertheim TPT1 using an effective number of tangent spheres  $m_{ef}$ . All interaction sites associated to each carbon atom had a hard sphere of diameter  $d=3.7109$  Å.

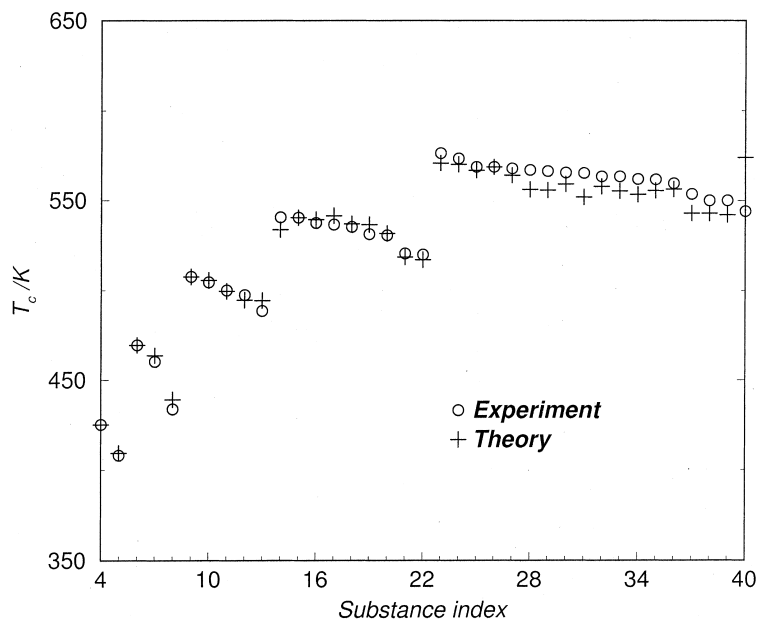


Fig. 3. Critical temperatures for butane, pentane, hexane, heptane and octane isomers. For each group of isomers, the experimental critical temperatures are arranged in decreasing order and compared with the corresponding (rescaled) theoretical results. The integer index associated to each alkane is described in detail in Ref. [28]. For each isomer both the experimental and the theoretical (from the perturbation theory described in the main text) critical temperatures are presented.

$n$ -hexane, while  $T_i^{\text{the}}$  is the theoretical prediction for isomer  $i$ .

In Fig. 3 the experimental critical temperatures [22] for a number of alkanes with up to eight carbon atoms are compared to those obtained from the rescaled theoretical predictions. For each group of isomers, the experimental critical temperature of a given alkane in that group is plotted in order of decreasing temperature, and the corresponding prediction from the theory is plotted for the same value of the abscissa. The figure shows rather good agreement with the experimental results. We note that whereas the apparent quantitative agreement results from rescaling, the qualitative agreement, i.e. ordering of the critical temperatures, is implicit in the theory. Particularly, it is seen that the theory is able to order correctly from high to low the critical temperatures of all isomers of butane, pentane and hexane, despite the fact that the differences between them amount to a few Kelvin. For heptane and octane isomers the agreement is less satisfactory but still rather reasonable.

Similar plots for the critical molar volume and pressure are shown in Figs. 4 and 5, respectively (i.e. the experimental properties are represented in decreasing order and the theoretical predictions are rescaled as in Eq. (16)). The agreement is seen once more to be rather good, and the decreasing trend in the critical volumes and pressures is found to be well captured, though, admittedly, the theory is not able to predict the correct ordering for all the substances. Such a possibility is

beyond our ability as a consequence of (1) our ignorance on the exact force field of each molecule, (2) the description of the structure by a simple mean field term and (3) the truncation of the perturbation expansion. This work shows, however, that a good quantitative theory may be expected by improving the description of the perturbation contribution. The advantage of the simple van der Waals approach is that it allows for a rationalization of the dependence of the critical parameters on the molecular properties. Indeed, by differentiation of the free energy, one finds that the pressure of the proposed equation of state takes the form:

$$p = p_{\text{MWT}}(\rho; \mathcal{Z}, \alpha) - a_{\text{vdw}} \rho^2 \quad (17)$$

where  $p_{\text{MW}}$  is the pressure as predicted by the MW equation of state. If we then apply the conditions for the critical point, we find that the critical properties may be obtained in a closed form in terms of three molecular parameters, namely,  $\mathcal{Z}$ , the molecular volume,  $\alpha$ , the non-sphericity, and  $a_{\text{vdw}}$ , the van der Waals constant:

$$V_c = \mathcal{Z} V_c^*(\alpha) \quad (18)$$

$$T_c = \frac{a_{\text{vdw}}}{k_B \mathcal{Z}} T_c^*(\alpha) \quad (19)$$

$$p_c = \frac{a_{\text{vdw}}}{\mathcal{Z}^2} p_c^*(\alpha) \quad (20)$$

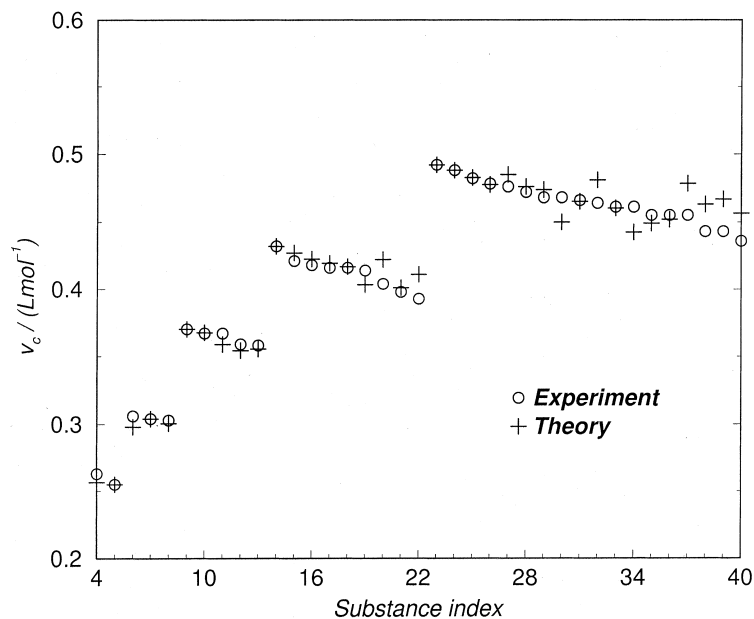


Fig. 4. As in Fig. 3 for the critical molar volumes.

where  $V_c^*$ ,  $T_c^*$  and  $p_c^*$  are all dimensionless, universal functions of  $\alpha$ . The explicit form of these functions is not important. What matters is that  $V_c^*$  is a monotonically increasing function of  $\alpha$ , while  $T_c^*$  and  $p_c^*$  are both monotonically decreasing functions of  $\alpha$  [44]. This knowledge is sufficient to use Eqs. (18)–(20) to make simple qualitative predictions on the variation of the critical properties in terms of the molecular parameters. As an example, Eq. (19) shows that the smaller  $\alpha$ , the larger  $T_c$ . This explains why highly branched alkanes

such as 2,3,3-trimethyloctane may have a larger critical temperature than *n*-octane, when it is expected that the former should have a smaller van der Waals constant. Table 2 presents a summary of the conclusions drawn from these equations.

### 3. The freezing transition of chain molecules

In this section we will consider the freezing of chain molecules made up of either tangent hard spheres or

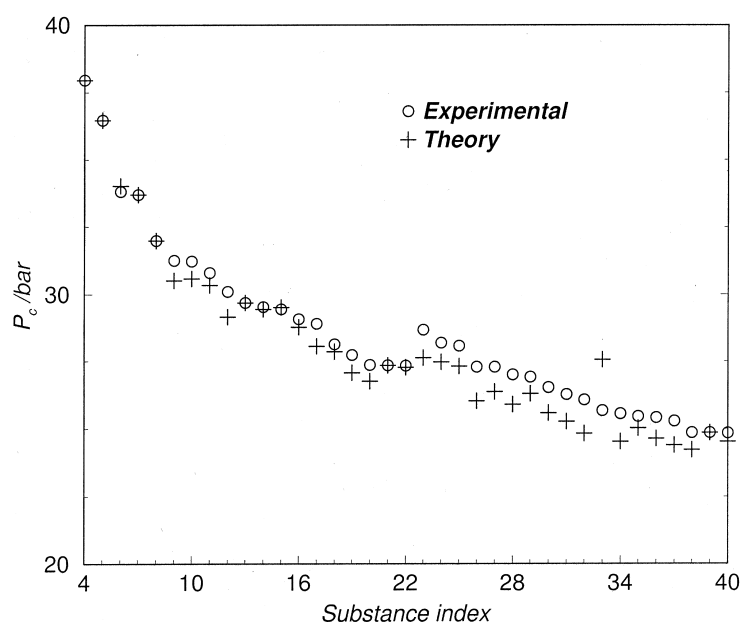


Fig. 5. As in Fig. 3 for the critical pressures.

Table 2  
Dependence of the critical properties with the molecular parameters as predicted from the van der Waals theory of this work

Critical property	Molecular parameter		
	$\alpha$	$\mathcal{V}$	$a_{\text{vdw}}$
$V_c$	↗	↗	—
$T_c$	↘	↘	—
$p_c$	↘	↘	—
$Z_c$	↘	—	—

‘↗’ and ‘↘’ indicate increase or decrease of the given property with respect to an increase in the corresponding molecular parameter, while ‘—’ indicates no dependence on that property.

Lennard–Jones chains. For the former, the reference potential is a simple hard sphere potential and the bond length  $\ell = d$  is set to the hard sphere diameter. For the latter, the interaction sites are LJ beads, and the bond length is set to  $\ell = \sigma$ . Note that for both systems,  $y(\ell) = g(\ell)$ , so that the background correlation function is substituted by the radial correlation function in Eqs. (1) and (2).

Let us analyze in more detail the information required to implement Wertheim’s theory for the solid phase. Let us start with hard spheres chains. For hard sphere chains, we need to know the EOS, residual free energy and contact value of the pair correlation function of the hard sphere monomer in the solid phase. This information had long been available. In fact, Hall [45] proposed an EOS for the hard sphere monomer in the solid phase that reproduces quite well the simulation results of hard spheres [46]. The contact value of  $g(\sigma)$  is obtained easily from the EOS of the hard sphere solid by using the virial theorem. The free energy of hard spheres in the solid phase can be obtained by thermodynamic integration of the EOS if the free energy is known at a reference point. The free energy of the hard sphere solid at a certain reference density was reported long ago by Hoover and Ree [47], and more recently by Polson et al. [48]. In summary all the information required to implement Wertheim’s theory for the solid phase of hard chains is available. What about LJ chains? For LJ chains, van der Hoef [49] has recently proposed an analytical expression, which reproduces almost exactly the simulation values of the free energies of the LJ solid. By differentiating the free energy expression with respect to density the EOS of the monomer LJ in the solid phase is obtained. The contact value of  $g(\sigma)$  for the LJ monomer was not available in the literature. However, we recently performed a number of computer simulations to determine  $g(\sigma)$  for the LJ monomer system in the solid phase and proposed an expression to fit all the simulation results [25]. Therefore, Wertheim’s theory can be applied to LJ chains. The third example is that of two-dimensional hard chains. For two-dimensional hard disks a good EOS for the monomer solid phase is

available [50]. By using the virial theorem in two dimensions the contact value of  $g(\sigma)$  can be obtained. Free energies of the two-dimensional hard disk have also been reported. Again all the ingredients needed to implement Wertheim’s theory for two-dimensional hard disk chains are available. Therefore the information required to implement Wertheim’s TPT1 to the solid phase of hard chains, LJ chains in three dimensions and hard disk chains in two dimension is available. The next natural question, is the following: what is the stable solid structure of hard sphere chains, LJ chains and hard disk chains?

Let us briefly discuss the solid structure of fully flexible tangent chains. For this model there is no energetic penalty when the atoms of the chains adopt a close-packed structure (for instance the face centered cubic fcc close-packed structure) with an ordered arrangement of atoms but with no long-range orientational order in the bond vectors of the chains. Wojciechowski et al. [51,52] were the first to realize this important feature in a continuum hard two-dimensional model. In fact Wojciechowski et al. [51,52] showed that the stable solid structure of tangent hard-disc dimers in two dimensions is formed by a close-packed arrangement of atoms with a disordered arrangement of bonds. The same idea holds for hard chains in three dimensions [53], and one may expect that the same would occur for a three-dimensional LJ chain. The bond disorder means that there is an additional contribution to the entropy of the system arising from the degeneracy of the structure.

As we have all of the information required, we shall now present computer simulation results for the free energy of hard sphere tangent dimers and for LJ tangent dimers, and proceed to compare directly the free energies obtained from simulation to those obtained from Wertheim’s TPT1 in the solid phase. This is certainly a severe test of the theory.

### 3.1. The hard dimer solid

In order to evaluate the fluid solid equilibrium of the hard dumbbell model, it is necessary to know the free energy of the disordered solid structure. For that purpose we have performed free energy calculations using the Einstein Crystal method proposed by Frenkel and Ladd [54]. Typically we used  $N=432$  molecules, with ten values of the spring constants ranging from 0 to  $\sigma^2\lambda_t/(kT)=4\times 10^3$  for the translational spring and from 0 to  $\lambda_r/(kT)=4\times 10^3$  for the orientational spring. The methodology of the Einstein crystal calculation used here is similar to that described in Ref. [26] and we refer the reader to this paper for further details. The reduced number density chosen for the free energy calculations was  $\rho^*=(N/V)\sigma^3=0.5490$ . This is not too far from the

expected density of the solid at melting. We performed free energy calculations for four different configurations of the disordered solid. In this way we were able to determine the free energy for each ‘individual’ configuration. Free energy differences between individual configurations of the disordered solid were found to be less than 0.5%. The average free energy of those individual configurations was found to be  $A/(NkT) = 11.36(0.02)$ . For comparison, the free energy of the dumbbell in the ordered solid structure, which will be denoted as CP1, has been calculated in Ref. [26] for the reduced density  $\rho^* = 0.5490$  and found to be  $A/(NkT) = 10.80$  [26]. This last result is obtained by thermodynamic integration from the free energy at  $\rho^* = 0.590$ , which is known from previous work.<sup>1,26</sup>

As it can be seen, for  $\rho^* = 0.5490$  the free energy of the ordered solid ( $A/(NkT) = 10.80$ ) is somewhat smaller than the average free energy of an individual disordered solid configuration ( $A/(NkT) = 11.36(0.02)$ ). However, there is an additional term to the free energy of the disordered solid that has not yet been included and which is not present in the ordered solid. In reality, the disordered solid has an additional free energy contribution arising from the fact that one must account for all the possible disordered arrangements of molecules compatible with the solid phase (i.e. number of ways in which the bonds may be arranged within the fcc lattice). This additional term to the free energy is usually denoted as the degeneracy entropy. The degeneracy entropy of a dimer on a fcc lattice has been estimated by several authors, and the best estimate ( $A/(NkT) = -1.5194$ ) is that of Nagle [55] (this number can also be obtained from the combinatorial entropy of mixing of the Flory–Huggins theory with a coordination number of 12). Therefore for the disordered solid the total free energy at  $\rho^* = 0.5490$  is given by  $A/(NkT) = 11.36 - 1.52 = 9.84(0.02)$ , thus showing that the stable solid phase is in fact the disordered solid. Notice that this result holds also in two dimensions, as first proved by Wojciechowski et al. [52]. The summary of the free energy calculations of the hard dimer for  $\rho^* = 0.5490$  can be found in

<sup>1</sup> Note that in this work we have used the hard sphere diameter as unit of length, whereas we used the diameter of a hard sphere with equal volume as the dimer in Ref. [26]. Since the free energies include an ideal gas term of the form  $\ln(\rho^*)$ , this means that there is a trivial  $\ln 2$  difference between the free energies of this work and those of Ref. [26]. Of course this does not affect coexistence densities but just the absolute values of the free energies.

Table 3

Helmholtz free energies (in  $NkT$  units) for the hard dumbbell model consisting of two tangent hard spheres

Method	Structure	$A_{\text{Einstein crystal}}/(NkT)$	Degeneracy	$A/(NkT)$
Simulation	Disordered solid	11.36 (2)	-1.5194	9.84 (2)
Simulation	Ordered CP1 solid	10.80	0	10.80 (3)
Theory	Disordered solid	*	*	9.76

The results correspond to the dimer at  $\rho^* = 0.5490$  in the disordered solid, and in the ordered solid labeled as CP1 in Ref. [26]. The free energies were obtained from simulation or from Wertheim’s TPT1 theory of the solid phase.

Table 4

Simulation results for the equation of state of hard dumbbells (two tangent hard spheres) in the disordered solid phase as obtained from NpT simulations

$\rho\sigma^3/kT$	$\rho^*$
60	0.6675
55	0.6648
50	0.6620
45	0.6556
40	0.6500
35	0.6420
30	0.6340
25	0.6205
20	0.6007
18	0.5917
16	0.5784
14	0.5645
12	0.5449
10	0.5166
8	0.4495
6	0.4189
4	0.3764
3	0.3463
2	0.3035
1.8	0.2930

The results correspond to the average of four independent configurations. For pressures below those of the empty line the solid is mechanically unstable and melts into an isotropic fluid.

Table 3, which also includes predictions from Wertheim’s theory. It is seen that for  $\rho^* = 0.5490$ , TPT1 predicts a free energy of  $A/(NkT) = 9.76$ , which is comparable with the simulation result,  $A/(NkT) = 9.84(0.02)$ . We point out that in order to obtain the free energy of the disordered solid from simulations one must first use the Einstein crystal methodology to obtain the free energy of individual configurations and then add the degeneracy contribution (i.e. the number of possible disordered structures). On the contrary, in Wertheim’s theory the degeneracy contribution is included implicitly. A similar procedure to that described here for three-dimensional hard dumbbells has been used by Wojciechowski et al. for the two-dimensional dimer problem [52].

In Table 4 the EOS for the disordered dumbbell solid as obtained from the Monte Carlo simulations of this work is presented. Simulation results were obtained using NpT ensemble. We used  $N = 432$  molecules with  $4 \times 10^4$  cycles for equilibration followed by another  $4 \times 10^4$  cycles for average production. A cycle involved

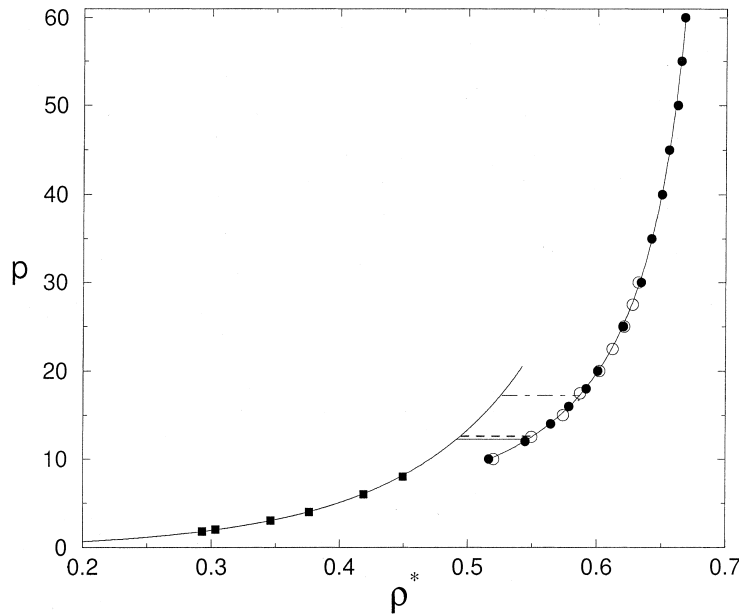


Fig. 6. Equation of state for hard dimers. Filled squares are simulation results for the fluid phase. Circles are results for the ordered (empty) and disordered (filled) solid phases. The dash-dotted line and the thick-dashed line are tie lines from simulation for the coexistence of fluid with ordered and disordered solid phases, respectively. The full lines are results from TPT1, with the tie line corresponding to the fluid-disordered solid coexistence. The pressure is given in  $kT/\sigma^3$  units.

a trial move per particle (translation or rotation) and a trial attempt of changing the volume of the system. The acceptance ratio was kept close to 30% for translational, rotational and volume changes. Results presented in Table 4 correspond to the average of the EOS obtained for four different configurations of the disordered solid. All pressures of this work are given in  $kT/\sigma^3$  units. The simulations began at the highest pressure, which was then slowly decreased. For pressures below 10 the disordered solid became mechanically unstable and melted into an isotropic fluid. The line in Table 4 separates the simulation results of the solid from those of the fluid phase.

In Fig. 6 we present simulation results for the EOS of the fluid, ordered solid and disordered solid, together with predictions from Wertheim's theory for the fluid and solid phases. The first thing to be noted from Fig. 6 is that the EOS of the ordered CP1 and disordered solid are quite similar, as already suggested some time ago [26]. Also, Sear and Jackson assumed that the EOS of the ordered solid was similar to that of the disordered one, when they first proposed a TPT1 like treatment for the dimer in the solid phase [56]. It is also clear from Fig. 6 that Wertheim's theory is able to describe quite well the fluid and solid branches of the dumbbell model. Not only that but also the agreement between theory and simulations for the location of the fluid solid equilibrium is quite good. In fact, according to the simulation results of this work the fluid–solid coexistence of the dumbbell model occurs for  $\rho_f^* = 0.4950$ ,  $\rho_s^* = 0.5525$ ,  $p = 12.62$  and  $\mu/(kT) = 32.82$ . However,

Wertheim's theory predicts  $\rho_f^* = 0.4915$ ,  $\rho_s^* = 0.5470$ ,  $p = 12.24$  and  $\mu/(kT) = 32.06$  in quite good agreement. The coexistence pressure as determined from our free energy calculations  $p = 12.62$  is consistent with the fact that the disordered solid becomes mechanically unstable for pressures below  $p = 10$ . In Fig. 6 the transition fluid-CP1 ordered solid is also presented. As can be seen the fluid-CP1 ordered solid occurs at a higher pressure (i.e.  $p = 17.28$ ) than the fluid-disordered solid transition ( $p = 12.62$ ). Therefore the fluid-ordered solid CP1 transition never occurs.

In Fig. 7, coexistence densities for the fluid–solid equilibrium of flexible chains are plotted as a function of  $m$  (the number of monomers of the chain). Simulations results for  $m = 1$  are taken from Ree and Hoover [47], those for  $m = 2$  from this work, and those for  $m = 3$  up to  $m = 8$  from Malanoski and Monson [53]. Lines correspond to theoretical predictions as obtained from Wertheim's theory for the fluid and solid phases. As can be seen, the agreement between theory and simulation is quite good. Similar good agreement is found in Fig. 8 for the coexistence pressure of hard sphere chains.

To summarise, we have shown that the stable solid for the dumbbell dimer is a disordered one, and that Wertheim's theory is able to yield a good description of the EOS and free energies of the disordered solid.

### 3.2. The two center Lennard–Jones dimer

For the two center Lennard–Jones model (2CLJ) we have performed free energy calculations for two different

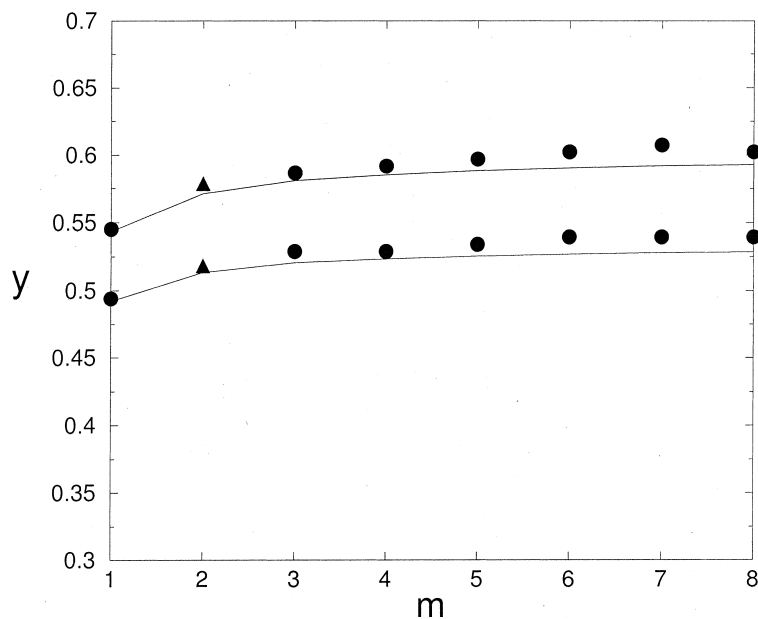


Fig. 7. Fluid and solid coexistence packing fractions as a function of chain length  $m$  (the solid phase refers to the disordered phase) for fully flexible tangent hard sphere chains. The filled circles are simulation results from Malanoski and Monson [53], the filled triangles are simulation results from this work. Full lines are theoretical predictions from TPT1.

reduced temperatures  $T^* = kT/\varepsilon$ , namely  $T^* = 1$  and  $T^* = 2$ . In both cases we used fifteen different values for the translational and rotational spring constants ranging from 0 to  $2 \times 10^4$ . The densities considered where  $\rho^* = 0.5490$  for  $T^* = 1$  and  $\rho^* = 0.5800$  for  $T^* = 2$ . The site–site pair potential was truncated at  $r = 2.5\sigma$  and long range corrections were added to the internal

energy (when the volume was changed these long range corrections were included within the Markov chain). Details of the calculations are similar to those described by Vega and Monson [57]. For the ordered CP1 structure we employed 256 molecules, while for the disordered structure we used 432 molecules. As for the hard sphere dimers, calculations were performed for four different

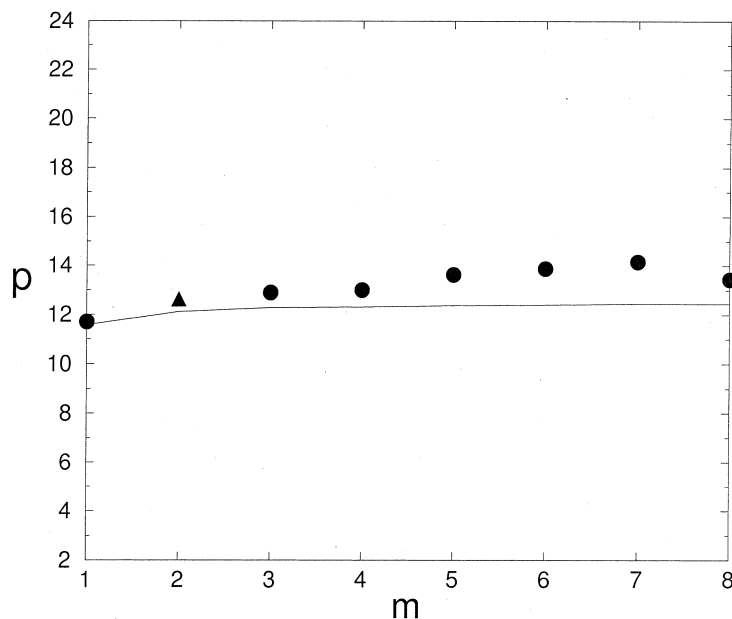


Fig. 8. Coexistence pressures for the fluid-disordered solid transition of fully flexible tangent hard sphere chains as a function of chain length. Symbols as in Fig. 7. The pressure is given in  $kT/\sigma^3$  units.

Table 5  
Helmholtz free energies as obtained from simulation for the 2CLJ at  $\rho^*=0.5490$  and  $T^*=1$

Method	Structure	$A_{\text{Einstein crystal}}/(NkT)$	Degeneracy	$A/(NkT)$
Simulation	Disordered solid	-4.17 (3)	-1.5194	-5.69 (3)
Simulation	Ordered CP1 solid	-4.76 (3)	0	-4.76 (3)
Theory	Disordered solid	*	*	-5.69

Results for the disordered solid and the ordered solid (denoted as CP1 in Ref. [26]). Results from Wertheim TPT1 theory are also presented.

configurations of the disordered solid. Results presented here correspond to the average of those disordered configurations. The final value of the free energy of the 2CLJ disordered solid was obtained by adding the degeneracy contribution  $-1.5194$  to the free energy calculations obtained from the Einstein crystal method.

Results from the free energy calculations for  $T^*=1$  are presented in Table 5. As can be seen the Einstein crystal energy of the ordered structure is smaller than that of the disordered solid. However, once the degeneracy entropy is added, the free energy of the disordered solid becomes smaller. Therefore for LJ dimers the disordered solid structure is also the most stable one. In Table 5 the prediction of Wertheim's theory for the free energy of the solid is also presented. As can be seen the agreement between theory and simulation is impressive. In a previous paper we have shown that Wertheim's theory gives quite good results for the EOS and internal energy of the solid disordered phase [25]. In this paper we show for the first time that the agreement for the free energy is also excellent. In Fig. 9 the free energy of the LJ dimer disordered solid is shown as obtained

from simulation and from Wertheim's theory for  $T^*=1$ . The free energy from simulation was obtained from the free energy at  $\rho^*=0.5490$  and using thermodynamic integration with the EOS as obtained from NpT simulations. As can be seen, the agreement between theory and simulation is quite good. This proves that Wertheim's theory can be used with confidence to predict all properties, internal energy, EOS and free energy of the LJ disordered solid.

In Table 6 the free energy of the disordered solid at  $T^*=2$  and  $\rho^*=0.58$  as obtained from this work is shown. Results from Wertheim theory are also shown. As can be seen again, Wertheim's theory yields quite good predictions of the free energy of the disordered solid, although the agreement is slightly worse than for  $T^*=1$ .

#### 4. Conclusions

In this paper we have shown how Wertheim's TPT1 theory can be used successfully to describe systems for which the theory was not originally designed. The two

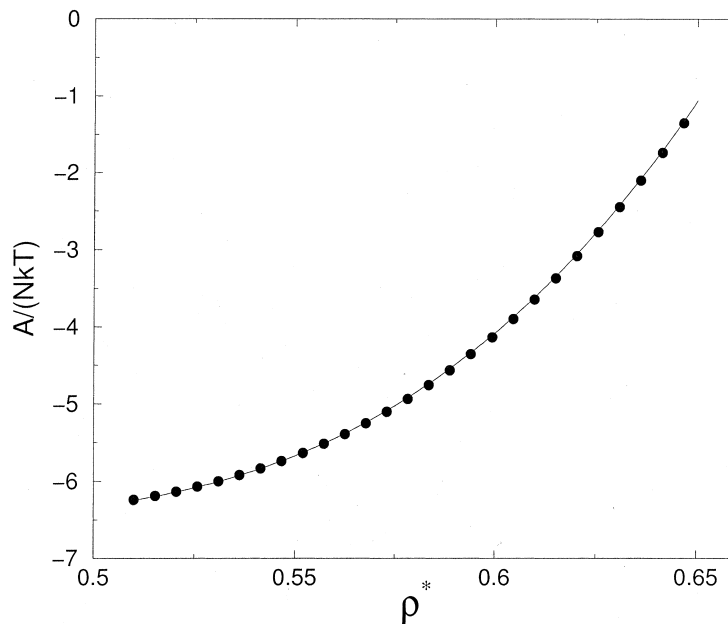


Fig. 9. Helmholtz free energy as a function of density for the disordered solid phase of the LJ dimer at  $T^*=1$ . Symbols, simulation results from this work; lines, theoretical predictions from TPT1. Due to a misprint the coefficient  $i=4, j=1$  of Table 1 of Reference [25] should read 69.219 (and not 68.219)

Table 6

Helmholtz free energies as obtained from simulation and from Wertheim TPT1 theory of the 2CLJ model at  $\rho^* = 0.580$  and  $T^* = 2$  in the disordered solid structure

Method	Structure	$A_{\text{Einstein crystal}}/(NkT)$	Degeneracy	$A/(NkT)$
Simulation	Disordered solid	3.13 (2)	-1.5194	1.61 (2)
Theory	Disordered solid	*	*	1.65

presented examples are, the description of realistic models of alkanes, linear and branched, and the description of flexible molecules in the solid phase. Main conclusions of this work are the following:

- Wertheim's TPT1 can be used to describe the EOS of realistic hard repulsive models of alkanes, by using the actual volume of the model, and an effective number of tangent spheres  $m_{ef}$ . This effective number can be obtained from the second virial coefficient of the hard model.
- Hard models of branched alkanes present a lower value of the compressibility (for a certain volume fraction) than the corresponding linear isomers. This behavior may be rationalized in terms of the non-sphericity factor,  $\alpha$ , since the compressibility increases linearly with  $\alpha$  at constant packing fraction and  $\alpha$  is found to decrease with branching.
- The mean field theory proposed in this work is able to capture the main trends in the critical properties of linear and branched alkanes.
- Wertheim's TPT1 theory can be used successfully to describe the solid phase of flexible models. This is true for tangent hard sphere models, and for tangent LJ models. In this work it has been shown that Wertheim's TPT1 yields free energies of the solid phase in excellent agreement with those obtained from simulation.
- We have proved by performing free energy calculations, that for the hard sphere and LJ dimer, the stable solid structure is one with an fcc arrangement of atoms, but with a disordered configuration of bonds.

## Acknowledgments

Financial support is due to project number FIS2004-06227-C02-02 and BFM-2001-1420-C02-02 of the Spanish DGES (Dirección General de Enseñanza Superior). L.G. MacDowell would like to thank the Spanish MCYT for the award of a Ramón y Cajal research grant. C. McBride would like to thank the European Union for the award of a post-doctoral Marie Curie Grant (HPMF-CT-1999-00163). E. Sanz would like to thank the Ministerio de Educación y Cultura for the award of a pre-doctoral grant. F.J. Blas would like to acknowledge the Universidad de Huelva and Junta de Andalucía for

additional financial support. A. Galindo would like to thank the Engineering and Physical Sciences Research Council for the award of an Advanced Research Fellowship.

## References

- [1] M.S. Wertheim, J. Stat. Phys. 35 (1984) 19.
- [2] M.S. Wertheim, J. Stat. Phys. 35 (1984) 35.
- [3] M.S. Wertheim, J. Stat. Phys. 42 (1986) 459.
- [4] M.S. Wertheim, J. Stat. Phys. 42 (1986) 477.
- [5] M.S. Wertheim, J. Chem. Phys. 85 (1986) 2929.
- [6] M.S. Wertheim, J. Chem. Phys. 87 (1987) 7323.
- [7] W.G. Chapman, G. Jackson, K.E. Gubbins, Mol. Phys. 65 (1988) 1057.
- [8] W.G. Chapman, J. Chem. Phys. 93 (1990) 4299.
- [9] J.K. Johnson, E.A. Müller, K.E. Gubbins, J. Phys. Chem. 98 (1994) 6413.
- [10] A. Gil-Villegas, A. Galindo, P.J. Whitehead, S.J. Mills, G. Jackson, A.N. Burgess, J. Chem. Phys. 106 (1997) 4168.
- [11] L.A. Davies, A. Gil-Villegas, G. Jackson, J. Chem. Phys. 111 (1999) 8659.
- [12] E.A. Müller, K.E. Gubbins, Ind. Eng. Chem. Res. 40 (2001) 2193.
- [13] F.J. Blas, L.F. Vega, Mol. Phys. 92 (1997) 135.
- [14] F.J. Blas, L.F. Vega, J. Chem. Phys. 115 (2001) 4355.
- [15] L.G. MacDowell, M. Müller, C. Vega, K. Binder, J. Chem. Phys. 113 (2000) 419.
- [16] Y. Zhou, G. Stell, J. Chem. Phys. 96 (1992) 1507.
- [17] W.R. Smith, I. Nezbeda, M. Strnad, B. Triska, S. Labik, A. Malijevsky, J. Chem. Phys. 109 (1998) 1052.
- [18] C. Vega, L.G. MacDowell, Mol. Phys. 98 (2000) 1295.
- [19] L.G. MacDowell, P. Virnau, M. Müller, K. Binder, J. Chem. Phys. 117 (2002) 6360.
- [20] D.A. McQuarrie, Statistical Mechanics, Harper and Row, New York, 1976.
- [21] C. Vega, L.G. MacDowell, J. Chem. Phys. 114 (2001) 10 411.
- [22] R.C. Reid, J.M. Prausnitz, B.E. Poling, The Properties of Gases and Liquids, 4th ed, MacGraw Hill, New York, 1987.
- [23] N. Elvassore, J.M. Prausnitz, Fluid Phase Equil. 194–197 (2002) 567.
- [24] C. McBride, C. Vega, J. Chem. Phys. 116 (2002) 1759.
- [25] C. Vega, F.J. Blas, A. Galindo, J. Chem. Phys. 116 (2002) 7645.
- [26] C. Vega, E.P.A. Paras, P.A. Monson, J. Chem. Phys. 96 (1992) 9060.
- [27] J. Rowlinson, F. Swinton, Liquids and Liquid Mixtures, 3rd ed, Butterworth, London, 1982.
- [28] L.G. MacDowell, C. Vega, J. Chem. Phys. 109 (1998) 5681.
- [29] J.P. Ryckaert, A. Bellemans, J. Chem. Soc. Faraday Discuss. 66 (1978) 95.
- [30] P.J. Flory, Statistical Mechanics of Chain Molecules, John Wiley & sons, New York, 1969.

- [31] C. Vega, S. Lago, B. Garzon, J. Chem. Phys. 100 (1994) 2182.
- [32] P. Padilla, C. Vega, Mol. Phys. 84 (1995) 435.
- [33] J.A. Barker, D. Henderson, J. Chem. Phys. 47 (1967) 4714.
- [34] T. Boublik, C. Vega, M.D. Peña, J. Chem. Phys. 93 (1990) 730.
- [35] J.M. Walsh, K.E. Gubbins, J. Phys. Chem. 94 (1990) 5115.
- [36] C. Vega, L.G. MacDowell, P. Padilla, J. Chem. Phys. 104 (1996) 701.
- [37] L.G. MacDowell, C. Vega, E. Sanz, J. Chem. Phys. 115 (2001) 6220.
- [38] E. Enciso, J. Alonso, N.G. Almarza, F.J. Bermejo, J. Chem. Phys. 90 (1989) 413.
- [39] N.G. Almarza, E. Enciso, F.J. Bermejo, Mol. Phys. 70 (1990) 485.
- [40] N.G. Almarza, E. Enciso, F.J. Bermejo, J. Chem. Phys. 96 (1992) 4625.
- [41] M.G. Martin, J.I. Siepmann, J. Phys. Chem. B 102 (1998) 2569.
- [42] L.G. MacDowell, C. Vega, J. Chem. Phys. 109 (1998) 5670.
- [43] A.P. Malanoski, P.A. Monson, J. Chem. Phys. 110 (1999) 664.
- [44] L.G. MacDowell, Ph.D. Thesis, Universidad Complutense de Madrid, 2000.
- [45] K.R. Hall, J. Chem. Phys. 57 (1972) 2252.
- [46] B.J. Alder, T.E. Wainwright, J. Chem. Phys. 33 (1960) 1439.
- [47] W.G. Hoover, F.H. Ree, J. Chem. Phys. 49 (1968) 3609.
- [48] J.M. Polson, E. Trizac, S. Pronk, D. Frenkel, J. Chem. Phys. 112 (2000) 5339.
- [49] M.A. van der Hoef, J. Chem. Phys. 113 (2000) 8142.
- [50] B.J. Alder, W.G. Hoover, D.A. Young, J. Chem. Phys. 49 (1968) 3688.
- [51] K.W. Wojciechowski, A.C. Branka, D. Frenkel, Phys. A 196 (1993) 519.
- [52] K.W. Wojciechowski, D. Frenkel, A.C. Branka, Phys. Rev. Lett. 66 (1991) 3168.
- [53] A.P. Malanoski, P.A. Monson, J. Chem. Phys. 107 (1997) 6899.
- [54] D. Frenkel, A.J.C. Ladd, J. Chem. Phys. 81 (1984) 3188.
- [55] J.F. Nagle, Phys. Rev. 152 (1966) 190.
- [56] R.P. Sear, G. Jackson, J. Chem. Phys. 102 (1995) 939.
- [57] C. Vega, P.A. Monson, J. Chem. Phys. 102 (1995) 1361.